

Article

Mesoporous CoO_x/C Nanocomposites Functionalized Electrochemical Sensor for Rapid and Continuous Detection of Nitrite

Xuhua Dong¹, Siqi Xie¹, Jingyang Zhu¹, Haiquan Liu¹, Yong Zhao¹, Tianjun Ni^{2,*}, Long Wu^{3,*}  and Yongheng Zhu^{1,*}

- ¹ Laboratory of Quality & Safety Risk Assessment for Aquatic Products on Storage and Preservation (Shanghai), College of Food Science and Technology, Ministry of Agriculture and Shanghai Engineering Research Center of Aquatic-Product Processing & Preservation Shanghai Ocean University, Shanghai 200120, China; xhdong5939@126.com (X.D.); 13651676832@163.com (S.X.); 15837688323@163.com (J.Z.); hqliu@shou.edu.cn (H.L.); yzhao@shou.edu.cn (Y.Z.)
- ² School of Basic Medicine, Xinxiang Medical University, Xinxiang 453003, China
- ³ National “111” Center for Cellular Regulation and Molecular Pharmaceutics, Key Laboratory of Fermentation Engineering (Ministry of Education), College of Bioengineering and Food, Hubei University of Technology, Wuhan 430068, China
- * Correspondence: tjni@xxmu.edu.cn (T.N.); longquan.good@163.com (L.W.); yh-zhu@shou.edu.cn (Y.Z.); Tel.: +86-0373-383-1859 (T.N.); +86-0898-6619-8861 (L.W.); +86-021-6190-0354 (Y.Z.)

Abstract: Nitrite is widespread in the environment, and is frequently used as an additive to extend the shelf life of meat products. However, the excess intake of nitrite can be harmful to human health. Hence, it is very important to know and control the content of nitrite in foodstuffs. In this work, by the means of self-assembly induced by solvent evaporation, we used the amphiphilic PEO-*b*-PS diblock copolymers resol and cobalt nitrate as a template to synthesize ordered mesoporous CoO_x/C nanocomposites. Then, the CoO_x/C nanocomposites were modified on a glassy carbon electrode (GCE), which showed excellent sensitivity, good selectivity, and a wide detection range for nitrite. Through cyclic voltammetry and current–time techniques, the electrochemical performance of the GCE modified with CoO_x/C nanocomposites was analyzed. Under the optimized conditions, we found that anodic currents were linearly related to nitrite concentrations with a regression equation of $I_p (\mu A) = 0.36388 + 0.01616C$ ($R^2 = 0.9987$) from 0.2 μM to 2500 μM , and the detection limit was 0.05 μM . Furthermore, the electrochemical sensor behaved with high reproducibility and anti-interference ability towards various organic and inorganic ions, such as NO₃[−], SO₄^{2−}, Cl[−], COOH[−] (Ac[−]), Na⁺, K⁺, Mg²⁺, and NH₄⁺. Our results indicated that these CoO_x/C nanocomposites could be applied in electrochemical sensors for the rapid and sensitive detection of the food preservative nitrite.

Keywords: nitrite; cobalt nanoparticles supported on ordered mesoporous carbon nanocomposites; electrochemical sensors



Citation: Dong, X.; Xie, S.; Zhu, J.; Liu, H.; Zhao, Y.; Ni, T.; Wu, L.; Zhu, Y. Mesoporous CoO_x/C Nanocomposites Functionalized Electrochemical Sensor for Rapid and Continuous Detection of Nitrite. *Coatings* **2021**, *11*, 596. <https://doi.org/10.3390/coatings11050596>

Received: 26 April 2021

Accepted: 14 May 2021

Published: 18 May 2021

Publisher’s Note: MDPI stays neutral with regard to jurisdictional claims in published maps and institutional affiliations.



Copyright: © 2021 by the authors. Licensee MDPI, Basel, Switzerland. This article is an open access article distributed under the terms and conditions of the Creative Commons Attribution (CC BY) license (<https://creativecommons.org/licenses/by/4.0/>).

1. Introduction

Nitrite is widespread in environmental, food, and life science, and is used as a preservative in food and in agricultural preservation to inhibit damage caused by foodborne pathogens, especially *Clostridium botulinum* [1]. However, the excess intake of nitrite is harmful to human health. In blood, nitrite can react with hemoglobin and cause hemoglobin oxidation, which brings about a disease known as “blue baby syndrome” [2]. In addition, nitrite can combine with amines to form nitrosamines, which have been shown to cause cancer as well as hypertension [3]. The reduction of the residual nitrite levels could be an acceptable alternative to reduce the intake of nitrite. At present, an increasing number of effective methods such as physical processing, chemical processing, and bio-enzymatic degradation have been applied for the abatement of nitrite compounds [4–7]. Due to

its potentially hazardous nature, the determination of nitrite is very important for human health and in the quality control of foods. Several common methods have been used to determine the content of nitrite, including spectrophotometry [8], chemiluminescence [9], chromatography [10], capillary electrophoresis [11], and so on. These methods can achieve good detection results for nitrite. However, they may have some shortcomings, such as complicated sample preparation processes, relatively low sensitivity and selectivity, high cost, and the requirement of specialized operations. Therefore, finding a simple, low-cost, and sensitive method for nitrite detection is essential to ensure food safety.

Owing to their advantages, such as low cost and direct on-site measurements, microfluidic paper-based analytical devices (μ PADs) and glass-based devices are also applied in the detection of nitrite [12–14]. Compared to the above-mentioned analytical methods, electrochemical techniques have many advantages, such as simple operation, low cost, good selectivity, fast response, excellent sensitivity, and no need for additional chemical reagents [15,16]. Nitrite is an electroactive substance with redox reaction at the surface of carbon electrodes, but the electron exchange rate is usually poor, which causes great limitations in the detection sensitivity [17]. It is reported that many nanostructured materials are excellent electrode materials with high conductivity [18–20]. Therefore, it is a good alternative approach to modify electrodes with these nanomaterials. For example, Wang et al. reported a paper-based disposable electrode for the detection of nitrite in environmental and food samples, taking advantage of the physicochemical properties of graphene nanosheets and gold nanoparticles [21]. Chen et al. constructed an electrochemical sensing platform for nitrite based on a Cu-based metal-organic framework (Cu-MOF) decorated with gold nanoparticles, which could ensure the stability of the platform and enhance its conductivity and catalytic activity [22]. However, these proposed methods failed to achieve either a relatively high sensitivity or a wide detection range. Therefore, it is urgent to develop other strategies to improve the electrochemical performance. It is well known that metal oxide nanoparticles/carbon nanomaterial hybrids can significantly enhance the performance of electrochemical sensors [23–26]. Metal oxides are often used as electrode materials due to their excellent electron transport rate. In order to achieve good electrocatalytic ability and chemical stability, cobalt oxides have often been used as modifiers of electrodes. For example, to detect nitrite sensitively, Haldorai et al. [25] proposed an electrochemical sensor modified with cobalt oxide (Co_3O_4) nanospindles-decorated reduced graphene oxide (RGO). Based on a cobalt monoxide (CoO)-nanoparticles-modified glassy carbon electrode (CS-CoO/GCE), Huang et al. [26] developed a new method which provided good catalysis and could improve the oxidation of the nitrite. Liu [27] synthesized a Co_3O_4 /RGO composite film immobilizing horseradish peroxidase, which exhibited excellent electrocatalytic activity toward nitrite. However, few studies have focused on metal oxide nanoparticles/ordered mesoporous carbon nanocomposites for nitrite detection. Owing to its large specific surface area, considerable pore volume, and adjustable pore size, ordered mesoporous carbon can make metal oxides evenly dispersed and highly active [28]. Furthermore, the physicochemical properties of the system can be enhanced by combining ordered mesoporous carbon with metal oxides, due to their synergistic effect.

There are many methods to synthesize ordered mesoporous carbon/metal oxides, including the post-loading method [29,30] and the direct synthesis method [31]. The post-loading method is carried out by preparing carbon materials and metal oxides separately, and then mixing them to obtain the nanocomposites. Meanwhile, the direct method uses a single process that can directly obtain the nanocomposites. Obviously, the direct synthesis method is easier and faster, which usually adopts a triblock copolymer as a template, combining a phenolic resin and metal salt precursors (metal nanoparticles) in the system, and then the target product of ordered mesoporous carbon/metal oxide is directly obtained by baking the template in an inert atmosphere [32]. Amphiphilic copolymers such as PEO-*b*-PS, PEO-*b*-PMMA, PEO-*b*-PHB, which have high molecular weight, have recently seen wide use as templates for the synthesis of ordered mesoporous materials with different compositions [33–37].

Hence, in this work, ordered mesoporous CoO_x/C nanocomposites were synthesized via a self-assembly method induced by solvent evaporation. After modifying an electrode with CoO_x/C nanocomposites, the glassy carbon electrode (GCE) showed excellent electrocatalytic activity for nitrite, which indicated that these nanocomposites could be applied in electrochemical sensors for the assessment of nitrite. When applying the sensor in experimental sausage samples, it obtained recoveries from 99.8% to 101.8%, further demonstrating the feasibility of the proposed method in practical samples.

2. Materials and Methods

2.1. Chemicals

Monomethyl poly (ethylene oxide) (CP; CAS No.: 75-21-8; 98.0%+) was obtained from Sigma-Aldrich (USA), with molar mass 5000 g/mol. N,N,N',N'',N'' -Pentamethyl diethylenetriamine (PMDETA) (CAS No.: 3030-47-5; 99.7%) was obtained from Acros Co., Ltd. (Beijing, China). Styrene (AR; CAS No.: 100-42-5), copper (I) bromide (CAS No.: 74774-53-1; 96.0%), Al_2O_3 (AR; CAS No.: 1344-28-1), and pyridine (AR; CAS No.: 110-86-1; 99.5%+) were purchased from Sinopharm Chemical Reagent Co. Ltd. (Shanghai, China). Cobalt nitrate hexahydrate (AR; CAS No.: 10026-22-9; 98.5%+), anhydrous ethyl ether (AR; CAS No.: 60-29-7; 99.7%+), tetrahydrofuran (THF) (AR; CAS No.: 109-99-9; 99.0%+), formalin solution (CAS No.: 50-00-0; 36.5-38%), phenol (AR; CAS No.: 108-95-2; 99.0%+), sodium hydroxide (AR; CAS No.: 1310-73-2; 96.0%+), and petroleum ether (30~60 °C; AR; CAS No.: 032-32-4) were obtained from Sinopharm Chemical Reagent Co. Ltd. (Shanghai, China). All chemicals were used as received without any further purification.

2.2. Synthesis of CoO_x/C Nanocomposites

According to a previously studied method [38], we synthesized the amphiphilic PEO-*b*-PS copolymers and soluble low-molecular-weight phenolic resin. The preparation method of the mesoporous CoO_x/C nanocomposites is depicted in Figure 1. In Step 1, the nanocomposites were synthesized in one step with the template method. To be specific, 0.08 g of $\text{Co}(\text{NO}_3)_2 \cdot 6\text{H}_2\text{O}$ was dissolved in 5 mL tetrahydrofuran (THF) which contained 0.4 g resol molecules. Then, the mixture was agitated for 0.5 h to obtain a transparent dark-red solution. After that, 0.1 g PEO-*b*-PS was dissolved in another 5 mL tetrahydrofuran (THF). Then, it was added dropwise into the above dark-red solution, with 2 h further stirring. To evaporate the tetrahydrofuran (THF), the solution was dropped on Petri dishes at 25 °C for 0.5 h. Following this, it was placed at 50 °C for 24 h to evaporate the solvent completely, and to fix the nanostructure via the thermal polymerization of resol, obtaining a yellow film as shown in Step 2. In Step 3, the yellow film was scraped off, and then ground into a powder in a tube furnace under N_2 atmosphere at 600 °C. Then, the final ordered mesoporous CoO_x/C nanocomposites could be obtained after the pyrolysis treatment. By adjusting the ratios, we obtained a series of samples and designated them as $\text{CoO}_x/\text{C-n}$, wherein n is the weight ratio of cobalt precursor to resol.

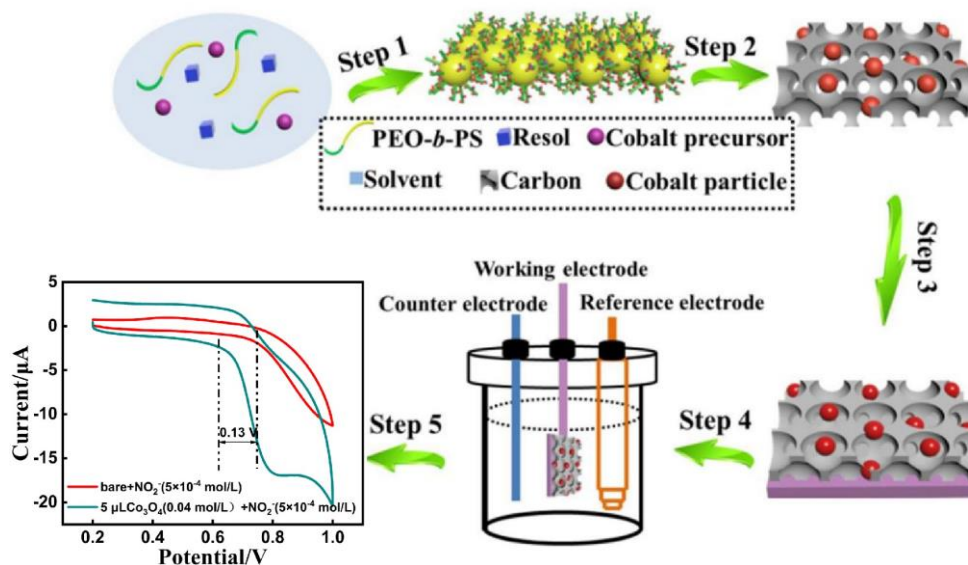


Figure 1. Schematic illustration of preparation of the ordered mesoporous CoO_x/C . Nanocomposites and modification of electrode for the nitrite detection.

2.3. Preparation of the Modified Electrode

Before modification, we polished the glassy carbon electrode (GCE) with alumina powder (grain size: 0.3 and 0.05 μm) successively. Next, the electrodes were sonicated with absolute alcohol and distilled water for 10~15 min respectively, and then dried in nitrogen environment. After that, a certain amount of the above CoO_x/C nanocomposite was dispersed in 1 mL water by ultrasonic stirring for 30 min, and then a homogenous suspension was obtained. Finally, a certain amount of the suspension was dropped on the surface of a GCE and dried in nitrogen environment.

2.4. Characterization and Measurements

Powder X-ray diffraction (XRD) patterns were recorded on a Bruker D4 X-ray diffractometer (Bruker, Karlsruhe, Germany) with Ni-filtered $\text{Cu K}\alpha$ radiation (40 kV, 40 mA). Transmission electron microscopy (TEM) images were taken on a JEM-2100 F microscope (JEOL, Tokyo, Japan) operated at 200 kV. The samples for TEM measurements were ultrasonically dispersed in absolute ethanol. Small-angle X-ray scattering (SAXS) measurements were employed using a Nanostar U small-angle X-ray scattering system (Bruker, Karlsruhe, Germany) with $\text{Cu K}\alpha$ radiation (40 kV, 35 mA).

All electrochemical measurements were performed using CHI 660D electrochemical workstation (Chenhua, Shanghai, China) with a conventional three-electrode system. The reference, working, and counter electrodes of the electrochemical sensor were modified by saturated calomel electrode (SCE), glassy carbon electrode (GCE), and a platinum foil, respectively.

3. Results and Discussion

3.1. Characterization

According to the scheme in Figure 1, through the solvent-evaporation-induced self-assembly method, we first synthesized a series of samples with different weight ratios (cobalt precursor/resol). SAXS and XRD were used to investigate their properties. As can be seen in Figure 2a, the samples of CoO_x/C -n-600 all had excellent diffraction peaks, suggesting that the ordered mesoporous structure can be formed at cobalt precursor/resol ratios from 0.1 to 0.3. In addition, CoO_x/C -0.2-600 exhibited the strongest diffraction peak, revealing that the ordered mesoporous structure was the best. However, the diffraction peaks were weaker for two other ratios of cobalt precursor to resol (CoO_x/C -0.1,

CoO_x/C-0.3), indicating that excessive or insufficient addition of cobalt precursor may affect the ordered structure. Figure 2b shows XRD measurements of the nanocomposites with different ratios of cobalt precursor/resol treated under N₂ atmosphere at 600 °C. As observed from the three curves, the distinct diffraction peaks appeared at 31.3, 36.9, 44.9, 59.6, and 65.4, corresponding to the Co₃O₄ cubic phase (JCPDS card no. 65-3103). The corresponding crystal planes were (220), (311), (400), and (440), respectively. This confirmed the presence of cobalt oxide on the ordered mesoporous carbon. Based on the pyrolysis treatment at 600 °C, cobalt valence changes were likely to happen [39–41].

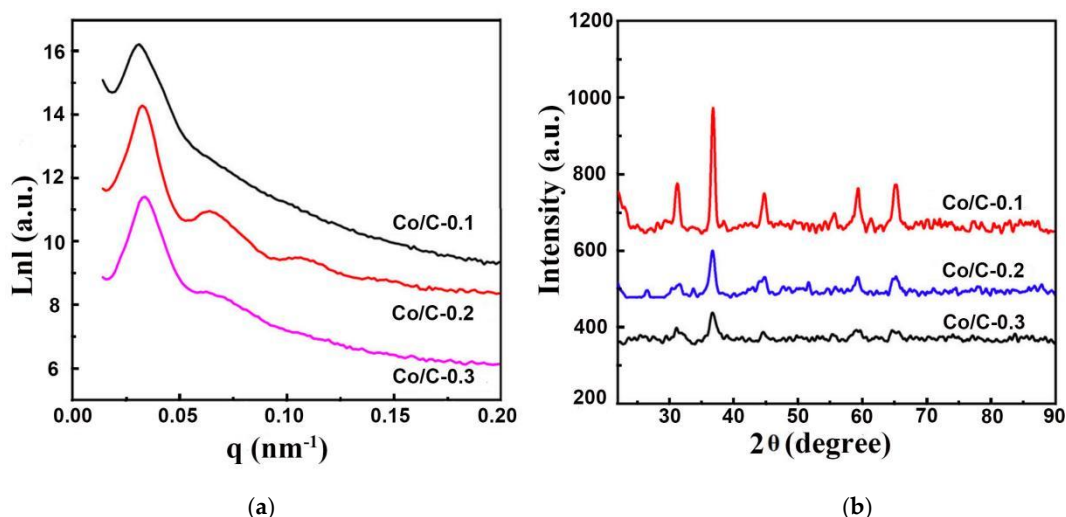


Figure 2. (a) SAXS patterns and (b) XRD measurements of the nanocomposites with different ratios of cobalt precursor/resol treated under N₂ atmosphere at 600 °C: CoO_x/C-0.1, CoO_x/C-0.2, CoO_x/C-0.3.

The appearances of the nanocomposites with different cobalt precursor/resol ratios were further examined by TEM. In Figure 3, it can be seen that the CoO_x nanoparticles were evenly distributed on the ordered mesoporous carbon nanocomposites. As the relative amount of cobalt precursor was increased, the size of the cobalt nanoparticles showed negligible changes, but the ordered pores in the mesoporous carbon were deteriorated. Especially, the ordered pores became the worst as excess CoO_x nanoparticles distributed on the ordered mesoporous carbon nanocomposites and the cobalt precursor/resol ratio reached 0.3. Considering the ordering of the material pores and the loading of cobalt precursor, we chose CoO_x/C-0.2 as the modifier on the electrode.

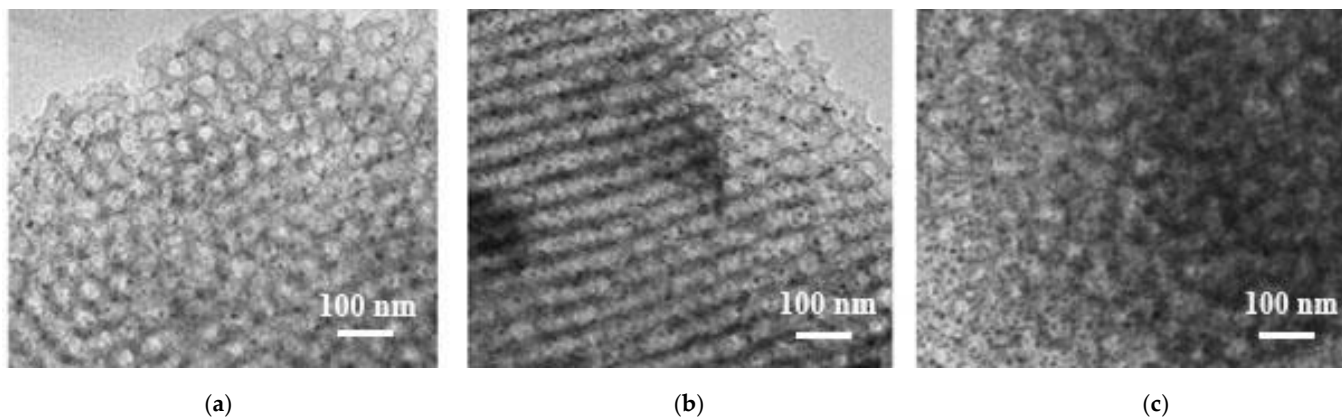


Figure 3. The TEM patterns of the nanocomposites with different cobalt precursor/resol ratio treated under N₂ atmosphere at 600 °C: (a) CoO_x/C-0.1; (b) CoO_x/C-0.2; (c) CoO_x/C-0.3.

3.2. Electrochemical and Catalytic Activity

The catalytic activity of a GCE modified with the ordered mesoporous CoO_x/C -0.2 nanocomposites was investigated by cyclic voltammetry (CV) and differential pulse voltammetry (DPV). Figure 4a shows that the CVs of the bare electrode and the GCE modified with the CoO_x/C -0.2 nanocomposites in 0.1 M PBS (pH = 3.5) showed responses to nitrite at the potential of 0.8 V. Furthermore, the bare electrode (curve 1) and the GCE modified with ordered mesoporous CoO_x/C -0.2 nanocomposites ($\text{CoO}_x/\text{C}@GCE$, curve 3) had no current of the oxidation peak in the 0.1 M PBS solution without nitrite. Additionally, the bare electrode showed an insignificant current of the oxidation peak in 0.1 M PBS containing 0.5 mM nitrite (curve 2). However, after modifying with ordered mesoporous CoO_x/C -0.2 nanocomposites, the GCE displayed an obvious current, with the oxidation peak located at 0.8 V (curve 4). These results indicate that nitrite oxidation may be catalyzed by the electron transport activity of the CoO_x/C -0.2 nanocomposites, which had excellent electrochemical and catalytic activity for nitrite.

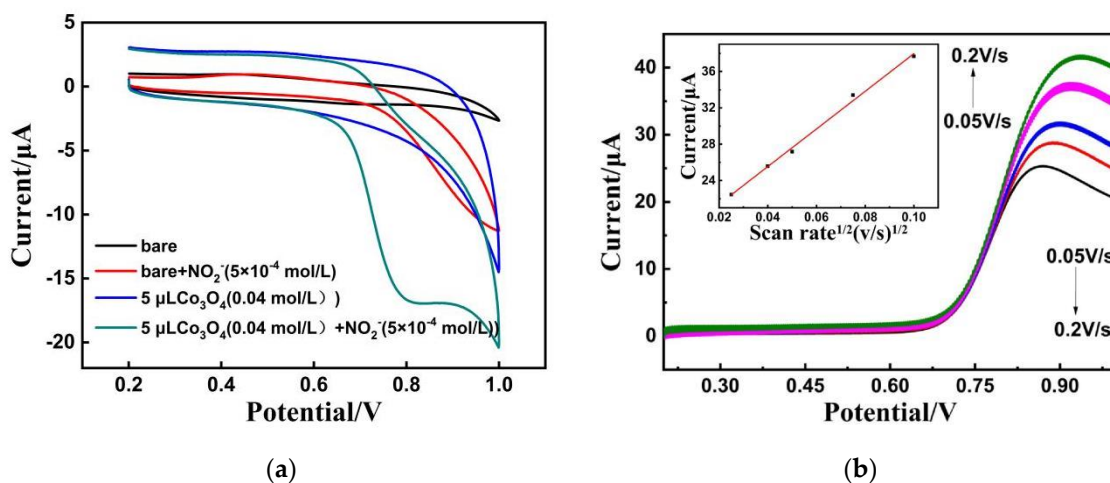


Figure 4. (a) CVs of bare electrode and GCE modified with ordered mesoporous CoO_x/C -0.2 nanocomposites in 0.1 M PBS (pH = 3.5) at 0.8 V potential (1: bare electrode; 2: bare electrode with 0.5 mM nitrite; 3: $\text{CoO}_x/\text{C}@GCE$; 4: $\text{CoO}_x/\text{C}@GCE$ with 0.5 mM nitrite). (b) DPVs of $\text{CoO}_x/\text{C}@GCE$ in 0.1 M PBS (pH = 3.5) and 1 mM nitrite at 0.8 V potential with scan rate from 0.05 to 0.2 $\text{V}\cdot\text{s}^{-1}$.

Further, Figure 4b shows the DPVs of $\text{CoO}_x/\text{C}@GCE$ in 1 mM nitrite and 0.1 M PBS (pH = 3.5) at 0.8 V potential with a scan rate of 0.05–0.2 $\text{V}\cdot\text{s}^{-1}$. There is a good linear relationship between the responding current and the square root of the scan rate. The magnitude of the current was proportional to the square root of the scan rate indicating that the electrode process was a diffusion-controlled process.

Experimental parameters can have a great influence on electrochemical sensor performance. Thus, the experimental conditions were optimized, including the applied potential, the volume of modifier, and the pH of the buffer solution. The optimized experimental conditions for applied potential, volume of modifier, and PBS pH were as follows: 0.8 V, 10 μL , pH = 3.5 of 0.1 M PBS (as shown in Figure S1).

With successive addition of nitrite, the amperometric responses were detected by the $\text{CoO}_x/\text{C}@GCE$ in 0.1 M PBS (pH = 3.5) at 0.8 V potential, under the optimal conditions. Figure 5 shows the typical amperometric response curves for different concentrations of nitrite. The currents responded to a wide detection range of nitrite concentrations, demonstrating the efficient catalytic property of the CoO_x/C -0.2 nanocomposites toward nitrite oxidation. Currents showed linear responses to nitrite concentrations from 0.2 μM to 2500 μM (Figure S2), which can be expressed with the regression equation $I_p (\mu\text{A}) = 0.36388 + 0.01616C$ ($R^2 = 0.9987$). When the signal-to-noise ratio was 3, the detection limit was 0.05 μM .

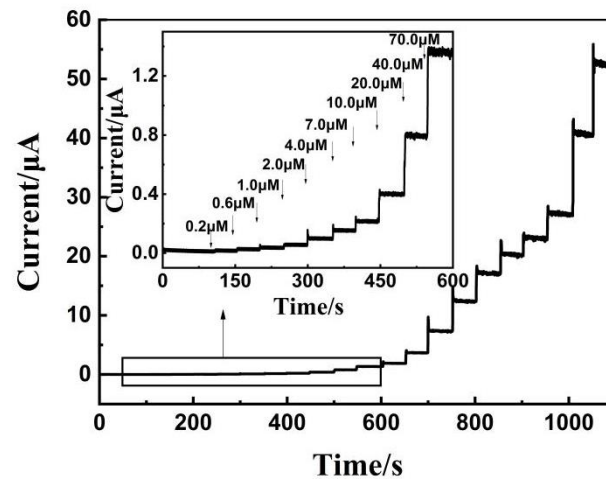


Figure 5. Typical current–time curves obtained by CoO_x/C@GCE at different concentrations of nitrite in 0.1 M PBS (pH = 3.5) at the potential of 0.8 V (inset: current–time responses for low concentrations from 0.2 to 70 µM).

3.3. Stability and Selectivity

Stability and selectivity are crucial indicators to evaluate the performance of electrochemical sensors. In the presence of 1 mM nitrite, the stability of the sensor was investigated by running 10 scans at 0.8 V in 0.1 M PBS (pH = 3.5). As shown in Figure 6a, the anodic peak current showed weak fluctuation after 10 scans, illustrating that the sensor had good stability within a certain range of detection. Additionally, we demonstrated the reproducibility of the sensor. To better reveal the reproducibility, five kinds of CoO_x/C-0.2 nanocomposites were synthesized and modified glassy carbon electrodes. The current signals of the five different electrodes gave a relative standard deviation of 3.86%, which exhibited good reproducibility. Furthermore, various interferences were added into 0.1 M PBS (pH = 3.5) containing 20 µM nitrite to verify the selectivity of the nitrite sensor. As shown in Figure 6b, a significant increase of current was observed when 20 µM nitrite was introduced, but no obvious current responses appeared when 2 mM NaNO₃, Na₂SO₄, KCl, MgSO₄, NH₄NO₃, or AcNa were introduced into the system at regular intervals. Therefore, this revealed that the nitrite sensor had an acceptable stability and reproducibility for nitrite detection, as well as an excellent anti-interference ability towards various organic and inorganic ions such as NO₃[−], SO₄^{2−}, Cl[−], COOH[−] and Na⁺, K⁺, Mg²⁺, NH₄⁺.

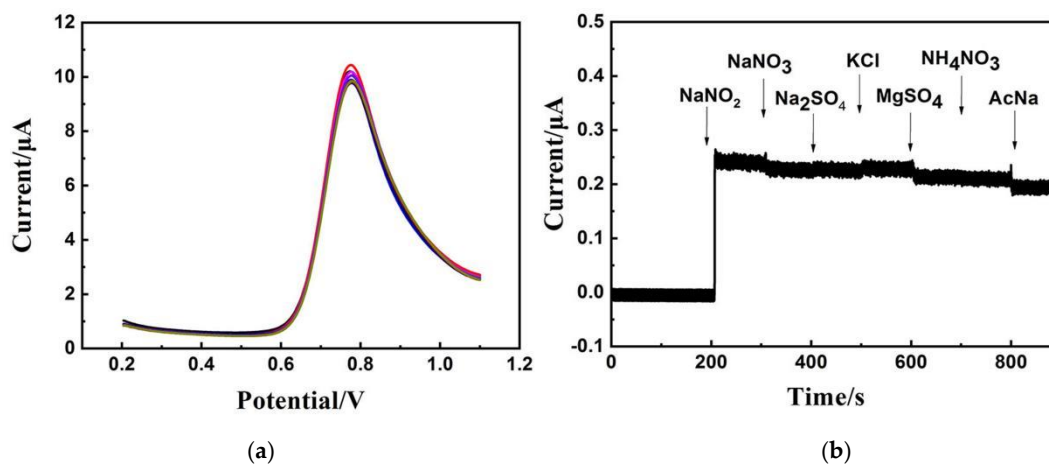


Figure 6. (a) Amperometric responses of CoO_x/C@GCE in 0.1 M PBS with 1 mM nitrite (pH = 3.5) at 0.8 V with 10 times scanning; (b) Amperometric responses of CoO_x/C@GCE on 20 µM nitrite and 2 mM interferences of NaNO₃, Na₂SO₄, KCl, MgSO₄, NH₄NO₃, and AcNa.

3.4. Application of the Sensor in Practical Food Samples

In order to evaluate the fabricated sensor's performance in real food samples, the sensor was used to detect the nitrite concentration in sausage samples. The sausage samples were obtained from a local market, and the pretreated samples were obtained according to the national standard [42] of operation. The accuracy of this proposed sensor was evaluated by a standard addition method. All the measurements were conducted under the optimal conditions of 0.1 M PBS (pH = 3.5) at 0.8 V using the current–time technique. The nitrite content in the sausage was measured to be 12.66 mg/kg, which is under the limited concentration set by national standard for food safety (20 mg/kg). As shown in Table 1, recoveries of the standard addition were 101.8%, 97.7%, and 99.8% for 5, 10, and 15 mg/kg added nitrite, respectively, which indicated that the proposed sensor had good performance for nitrite detection in sausage samples. The results also confirmed that the CoO_x/C-0.2 nanocomposites are very suitable for the construction of electrochemical sensors for the detection of nitrite in foods.

Table 1. Recovery studies of the proposed sensor in sausage samples.

Sample No.	NO ²⁻ Added (mg/kg)	NO ²⁻ Found (mg/kg)	Recovery (%)
1	5.00	17.75	101.8
2	10.00	22.43	97.7
3	15.00	27.63	99.8

4. Conclusions

In this work, we used amphiphilic PEO-*b*-PS, resol, and cobalt nitrate as templates to synthesize ordered mesoporous CoO_x/C nanocomposites in one step. With these CoO_x/C-0.2 nanocomposites, we fabricated a nitrite electrochemical sensor, which showed magnificent electrocatalytic activity for the nitrite. For nitrite, the sensor exhibited high selectivity, excellent sensitivity, and a wide detection range (from 0.2 μM to 2500 μM). The current responses to different nitrite concentrations showed a linear relationship, with the regression equation $I_p (\mu A) = 0.36388 + 0.01616C$ ($R^2 = 0.9987$). When the signal-to-noise ratio was 3, the detection limit was 0.05 μM. Moreover, the electrochemical sensor demonstrated good stability and reproducibility, which indicated that the ordered mesoporous CoO_x/C nanocomposites could be applied in electrochemical sensors for the detection of nitrite in food samples. Although we managed to develop a high-performance electrochemical sensor based on CoO_x/C nanocomposites, the electrochemical method is sensitive to the environment. Great attention should be paid to the influence of the nanomaterials and substrates on the signal outputs. Despite their various advantages, electrochemical methods suffer from shortcomings such as relatively low reproducibility and selectivity, short working life, and difficult reuse of the electrode and electrolyte. Therefore, there are still many remaining challenges to be solved in developing ideal electrochemical methods.

Supplementary Materials: The following are available online at <https://www.mdpi.com/article/10.3390/coatings11050596/s1>, Figure S1: Current response of CoO_x/C@GCE at different (a) applied potentials; (b) volume of modifier; (c) pH value of PBS. Figure S2: Calibrated curve between the amperometric responses and nitrite concentrations from 0.2 to 2500 μM.

Author Contributions: Conceptualization, Y.Z. (Yongheng Zhu); methodology, X.D. and L.W.; software, X.D.; validation, Y.Z. (Yongheng Zhu), L.W., X.D., and T.N.; formal analysis, X.D. and T.N.; investigation, X.D.; resources, Y.Z. (Yongheng Zhu) and H.L.; data curation, X.D.; writing—original draft preparation, X.D., S.X., and J.Z.; writing—review and editing, X.D., J.Z., and S.X.; visualization, X.D. and T.N.; supervision, Y.Z. (Yongheng Zhu) and L.W.; project administration, Y.Z. (Yongheng Zhu); funding acquisition, Y.Z. (Yongheng Zhu) and Y.Z. (Yong Zhao). X.D. and S.X. contributed equally. All authors have read and agreed to the published version of the manuscript.

Funding: This research was funded by the National Natural Science Foundation of China (31701678, 31801638), the Key Project of Shanghai Agriculture Prosperity through Science and Technology (2019-02-08-00-15-F01147), and the Key Science and Technology Project of Henan (No.172102310586). The authors sincerely thank all the panelists for experimental support.

Institutional Review Board Statement: Not applicable.

Informed Consent Statement: Not applicable.

Data Availability Statement: The data presented in this study are available on request from the corresponding author.

Conflicts of Interest: The authors declare no conflict of interest.

References

1. Wang, Q.; Yu, L.; Liu, Y.; Lin, L.; Lu, R.; Zhu, J.; He, L.; Lu, Z. Methods for the detection and determination of nitrite and nitrate: A review. *Talanta* **2017**, *165*, 709–720. [[CrossRef](#)] [[PubMed](#)]
2. Velmurugan, S.; Palanisamy, S.; Yang, T. Single-crystalline SnS₂ nano-hexagons based non-enzymatic electrochemical sensor for detection of carcinogenic nitrite in food samples. *Sens. Actuators B Chem.* **2020**, *316*, 128106. [[CrossRef](#)]
3. Chen, Y.; Zhao, C.; Yue, G.; Yang, Z.; Wang, Y.; Rao, H.; Zhang, W.; Jin, B.; Wang, X. A highly selective chromogenic probe for the detection of nitrite in food samples. *Food Chem.* **2020**, *317*, 126361. [[CrossRef](#)] [[PubMed](#)]
4. Mao, Q.; Deng, G.; Zou, C.; Xu, Y.; Cheng, W. Advances in Degradation Method for Nitrite in Vegetables. *Human Agric. Sci.* **2017**, *7*, 109–111.
5. Li, X.; Meng, X.; Li, J. Research progress on method for nitrite abatement in pickles. *J. Agric. Sci. Technol.* **2012**, *14*, 90–95.
6. Viuda-Martos, M.; Fernandez-Lopez, J.; Sayas-Barbera, E.; Sendra, E.; Navarro, C.; Perez-Alvarez, J. Citrus Co-Products as Technological Strategy to Reduce Residual Nitrite Content in Meat Products. *J. Food Sci.* **2009**, *74*, R93–R100. [[CrossRef](#)]
7. Liu, D.; Wang, P.; Zhang, X.; Xu, X.; Wu, H.; Li, L. Characterization of Nitrite Degradation by *Lactobacillus casei* subsp *rhamnosus* LCR 6013. *PLoS ONE* **2014**, *9*, e93308. [[CrossRef](#)]
8. Li, Y.; Zhao, C.; Li, B.; Gao, X. Evaluating nitrite content changes in some Chinese home cooking with a newly-developed CDs diazotization spectrophotometry. *Food Chem.* **2020**, *330*, 127151. [[CrossRef](#)]
9. Gill, A.; Zajda, J.; Meyerhoff, M. Comparison of electrochemical nitric oxide detection methods with chemiluminescence for measuring nitrite concentration in food samples. *Anal. Chim. Acta* **2019**, *1077*, 167–173. [[CrossRef](#)]
10. Zhang, S.; Peng, R.; Jiang, R.; Chai, X.; Barnesc, D. A high-throughput headspace gas chromatographic technique for the determination of nitrite content in water samples. *J. Chromatogr. A* **2018**, *1538*, 104–107. [[CrossRef](#)]
11. Wang, X.; Adams, E.; Schepdael, A. A fast and sensitive method for the determination of nitrite in human plasma by capillary electrophoresis with fluorescence detection. *Talanta* **2012**, *97*, 142–144. [[CrossRef](#)]
12. Ferreira, F.T.; Mesquita, R.B.; Rangel, A.O. Microfluidic paper-based analytical devices for the determination of salivary NOx. In Proceedings of the XXIV Encontro Luso-Galego de Química, Porto, Portugal, 21–23 November 2018; p. 330.
13. Maruo, Y.Y. Measurement of ambient ozone using newly developed porous glass sensor. *Sens. Actuators B Chem.* **2007**, *126*, 485–491. [[CrossRef](#)]
14. Veiko, V.P.; Zakoldaev, R.A.; Sergeev, M.M.; Danilov, P.A.; Kudryashov, S.I.; Kostiuk, G.K.; Medvedev, O.S. Direct Laser Writing of Barriers with Controllable Permeability in Porous Glass. *Opt. Express* **2018**, *26*, 28150–28160. [[CrossRef](#)] [[PubMed](#)]
15. Bansod, B.; Kumar, T.; Thakur, R.; Rana, S.; Singh, I. A review on various electrochemical techniques for heavy metal ions detection with different sensing platforms. *Biosens. Bioelectron.* **2017**, *94*, 443–455. [[CrossRef](#)] [[PubMed](#)]
16. Li, Z.; Mohamed, M.A.; Vinu Mohan, A.M.; Zhu, Z.; Sharma, V.; Mishra, G.K.; Mishra, R.K. Application of electrochemical aptasensors toward clinical diagnostics, food, and environmental monitoring. *Sensors* **2019**, *19*, 5435. [[CrossRef](#)] [[PubMed](#)]
17. Wu, L. Analysis of food Additives. In *Innovative Food Analysis*; Galanakis, C., Ed.; Academic Press: Pittsburgh, PA, USA, 2021; Volume 7, pp. 157–180.
18. Kabir, S.; Artyushkova, K.; Serov, A.; Atanassov, P. Role of nitrogen moieties in N-doped 3D-graphene nanosheets for oxygen electroreduction in acidic and alkaline media. *ACS Appl. Mater. Interfaces* **2018**, *10*, 11623–11632. [[CrossRef](#)]
19. Cai, Z.; Xiong, H.; Zhu, Z.; Huang, H.; Li, L.; Huang, Y.; Yu, X. Electrochemical synthesis of graphene/polypyrrole nanotube composites for multifunctional applications. *Synth. Met.* **2017**, *227*, 100–105. [[CrossRef](#)]
20. Pourmadadi, M.; Shayeh, J.S.; Omidi, M.; Yazdian, F.; Alebouyeh, M.; Tayebi, L. A glassy carbon electrode modified with reduced graphene oxide and gold nanoparticles for electrochemical aptasensing of lipopolysaccharides from *Escherichia coli* bacteria. *Microchim. Acta* **2019**, *186*, 1–8. [[CrossRef](#)] [[PubMed](#)]
21. Wang, P.; Wang, M.; Zhou, F.; Yang, G.; Qu, L.; Miao, X. Development of a paper-based, inexpensive, and disposable electrochemical sensing platform for nitrite detection. *Electrochem. Commun.* **2017**, *81*, 74–78. [[CrossRef](#)]
22. Chen, H.; Yang, T.; Liu, F.; Li, W. Electrodeposition of gold nanoparticles on Cu-based metal-organic framework for the electrochemical detection of nitrite. *Sens. Actuators B Chem.* **2019**, *286*, 401–407. [[CrossRef](#)]
23. Ding, S.; Li, X.; Jiang, X.; Hu, Q.; Yan, Y.; Zheng, Q.; Lin, D. Core-shell nanostructured ZnO@CoS arrays as advanced electrode materials for high-performance supercapacitors. *Electrochim. Acta* **2009**, *137*, 710–714.

24. Teymourian, H.; Salimi, A.; Khezrian, S. Fe₃O₄ magnetic nanoparticles/reduced graphene oxide nanosheets as a novel electrochemical and bioelectrochemical sensing platform. *Biosens. Bioelectron.* **2013**, *49*, 1–8. [[CrossRef](#)] [[PubMed](#)]
25. Haldorai, Y.; Kim, J.; Vilian, A.; Heo, N.; Huh, Y.; Han, Y. An enzyme-free electrochemical sensor based on reduced graphene oxide/Co₃O₄ nanospindle composite for sensitive detection of nitrite. *Sens. Actuators B Chem.* **2020**, *227*, 92–99. [[CrossRef](#)]
26. Huang, G.; Zhang, J.; Zhao, D. Cobalt monoxide nanoparticles modified glassy carbon electrodes as a sensor for determination of nitrite. *Adv. Mater. Res.* **2015**, *1120–1121*, 291–298. [[CrossRef](#)]
27. Liu, H.; Guo, K.; Lv, J.; Gao, Y.; Duan, C.; Deng, L.; Zhu, Z. A novel nitrite biosensor based on the direct electrochemistry of horseradish peroxidase immobilized on porous Co₃O₄ nanosheets and reduced graphene oxide composite modified electrode. *Sens. Actuators B Chem.* **2017**, *238*, 249–256. [[CrossRef](#)]
28. Wu, Z.; Zhao, D. Ordered mesoporous materials as adsorbents. *Chem. Commun.* **2011**, *47*, 3332–3338. [[CrossRef](#)]
29. Wu, Z.; Li, W.; Webley, P.; Zhao, D. General and controllable synthesis of novel mesoporous magnetic iron oxide@carbon encapsulates for efficient arsenic removal. *Adv. Mater.* **2020**, *24*, 485–491. [[CrossRef](#)] [[PubMed](#)]
30. Gu, D.; Li, W.; Wang, F.; Bongard, H.; Spliethoff, B.; Schmidt, W.; Weidenthaler, C.; Xia, Y.; Zhao, D.; Schüth, F. Controllable synthesis of mesoporous peapod-like Co₃O₄@Carbon nanotube arrays for high-performance lithium-ion Batteries. *Angew. Chem. Int. Ed.* **2015**, *54*, 7060–7064. [[CrossRef](#)] [[PubMed](#)]
31. Tang, J.; Wang, T.; Pan, X.; Sun, X.; Fan, X.; Guo, Y.; Xue, H.; He, J. Synthesis and electrochemical characterization of n-doped partially graphitized ordered mesoporous carbon–Co composite. *J. Phys. Chem. C* **2013**, *117*, 16896–16906. [[CrossRef](#)]
32. Sun, Z.; Sun, B.; Qiao, M.; Wei, J.; Yue, Q.; Wang, C.; Deng, Y.; Kaliaguine, S.; Zhao, D. A general chelate-assisted Co-assembly to metallic nanoparticles-incorporated ordered mesoporous carbon catalysts for fischer–tropsch synthesis. *J. Am. Chem. Soc.* **2020**, *134*, 17653–17660. [[CrossRef](#)]
33. Mohamed, M.; Atayde, E.; Matsagar, B.; Na, J.; Yamauchi, Y.; Wu, K.; Kuo, K. Construction hierarchically mesoporous/microporous materials based on block copolymer and covalentorganic framework. *J. Taiwan Inst. Chem. E* **2020**, *112*, 180–192. [[CrossRef](#)]
34. Luo, W.; Li, Y.; Dong, J.; Wei, J.; Xu, J.; Deng, Y.; Zhao, D. A Resol-assisted Co-Assembly approach to crystalline mesoporous niobia spheres for electrochemical biosensing. *Angew. Chem. Int. Ed.* **2013**, *52*, 10505–10510. [[CrossRef](#)]
35. Xiong, H.; Zhou, H.; Qi, C.; Liu, Z.; Zhang, L.; Zhang, L.; Qiao, Z. Polymer-oriented evaporation induced self-assembly strategy to synthesize highly crystalline mesoporous metal oxides. *Chem. Eng. J.* **2020**, *398*, 125527. [[CrossRef](#)]
36. Li, Y.; Luo, W.; Qin, N.; Dong, J.; Wei, J.; Li, W.; Feng, S.; Chen, J.; Xu, J.; Elzatahry, A.; et al. Highly ordered mesoporous tungsten oxides with a large pore size and crystalline framework for H₂S sensing. *Angew. Chem. Int. Ed.* **2014**, *53*, 9035–9040. [[CrossRef](#)]
37. Zhang, J.; Deng, Y.; Gu, D.; Wang, S.; She, L.; Che, R.; Wang, Z.; Tu, B.; Xie, S.; Zhao, D. Ligand-assisted assembly approach to synthesize large-pore ordered mesoporous titania with thermally stable and crystalline framework. *Adv. Energy Mater.* **2011**, *1*, 241–248. [[CrossRef](#)]
38. Wang, Z.; Zhu, Y.; Luo, W.; Ren, Y.; Cheng, X.; Xu, P.; Li, X.; Deng, Y.; Zhao, D. Controlled synthesis of ordered mesoporous carbon-cobalt oxide nanocomposites with large mesopores and graphitic walls. *Chem. Mater.* **2016**, *28*, 7773–7780. [[CrossRef](#)]
39. Bresser, D.; Paillard, E.; Niehoff, P.; Krueger, S.; Mueller, F.; Winter, M.; Passerini, S. Challenges of “going nano”: Enhanced electrochemical performance of cobalt oxide nanoparticles by carbothermal reduction and in situ carbon coating. *Chem. Phys. Chem.* **2014**, *15*, 2177–2185. [[CrossRef](#)]
40. Jin, H.; Wang, J.; Su, D.; Wei, Z.; Pang, Z.; Wang, Y. In situ cobalt-cobalt oxide/n-doped carbon hybrids as superior bifunctional electrocatalysts for hydrogen and oxygen evolution. *J. Am. Chem. Soc.* **2015**, *137*, 2688–2694. [[CrossRef](#)] [[PubMed](#)]
41. Wei, Z.; Wang, J.; Mao, S.; Su, D.; Jin, H.; Wang, Y.; Xu, F.; Li, H.; Wang, Y. In situ-generated Co⁰-Co₃O₄/n-doped carbon nanotubes hybrids as efficient and chemoselective catalysts for hydrogenation of nitroarenes. *ACS Catal.* **2015**, *5*, 4783–4789. [[CrossRef](#)]
42. GB 5009.33-2016. *Food Safety National Standard-Determination of Nitrite and Nitrate in Food*; The Standardization Administration of the People’s Republic of China: Beijing, China, 2016.